ACS OMEGA

http://pubs.acs.org/journal/acsodf

Article

Green Synthesis of Gold Nano-bioconjugates from Onion Peel Extract and Evaluation of Their Antioxidant, Anti-inflammatory, and Cytotoxic Studies

Kabyashree Phukan, Rajlakshmi Devi,* and Devasish Chowdhury*

Cite This: *ACS Omega* 2021, 6, 17811−17823

Read Online

ACCESS | Metrics & More | Article Recommendations

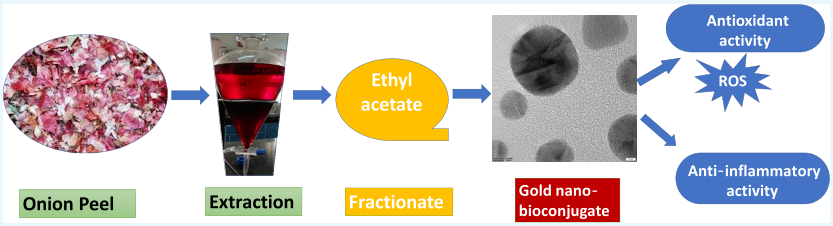

ABSTRACT: Plant secondary metabolites such as flavonoids demonstrate high degrees of antioxidant, anti-inflammatory, and anticancer activities. Among flavonoids, quercetin plays an important role in inflammation by downregulating the level of various cytokines. Thereby, in this work, onion (*Allium cepa*) peel was successfully utilized for the synthesis of gold nano-bioconjugates acting as a natural therapeutic drug. In this process, crude onion peel extract was first divided into different fractionates, namely, ethyl acetate, butanol, methanol, and water, and they were subjected to various preliminary studies of antioxidant activities. The ethyl acetate fractionate shows high antioxidant activities in all the assays. The bioactive components were identified and found to contain a high amount of quercetin as confirmed by liquid chromatography with tandem mass spectrometry and high-performance liquid chromatogrpahy. Three gold nano-bioconjugates were prepared with different concentrations of the ethyl acetate fractionate. Various biochemical anti-inflammatory assays were carried out and compared with the active ethyl acetate fraction of the onion peel drug (OPD). The cytotoxicity of the nano-bioconjugate system and the OPD was checked in the myoblast L6 cell line from skeletal muscle tissues to evaluate the toxicity. All the three nano-bioconjugates A, B, and E demonstrated high percentages of cell viability, viz., 73.07, 72.3, and 69.15%, respectively, at their highest concentration of 200 μg/mL. The OPD also showed 88.56% cell viability with no toxic effects in the myoblast L6 cell line from skeletal muscle tissues. The reactive oxygen species reduction of nano-bioconjugate B showed a marked reduction of 76.77% at a maximum concentration of 200 μg/mL, whereas the OPD showed 68.17%. Hence, through this work, a cheap source of nano-bioconjugates is developed, which can act as a potent antioxidant and anti-inflammatory agent and are more active in comparison to the OPD alone.

1. INTRODUCTION

Numerous NSAIDs (nonsteroidal anti-inflammatory drugs) are being used to reduce inflammation. These anti-inflammatory NSAIDs have various side effects that can be overcome by the alternative application of medicinal plants. Plant secondary metabolites are tremendously being used for decades in various therapeutic applications, such as cardiovascular diseases, cancers, and neurodegenerative diseases.[1] Many researchers have reported the antioxidant and anti-inflammatory activities of plant secondary metabolites and their application in the treatment of arthritis.[2] Cardiovascular diseases, cancers, and various autoimmune disorders are due to continuous and chronic inflammatory responses caused by the rapid generation of superoxide radicals and surplus activation of phagocytes.[3,4] Recently, researchers found interest in the plant metabolite content in onion (*Allium cepa*), which is a versatile vegetable, for various epidemiological studies that reveal that consumption of onion reduces the risk of cancers, diabetes, and various neurodegenerative diseases.[5−8] Onion is a rich source of biologically active compounds such as flavonoids, phenolics, and anthocyanins.[9]

Among other flavonoids, quercetin plays an important role in lipid peroxidation inhibition, scavenging oxygen radicals, and can alter various biochemical pathways.[10,11] Major phenolic compounds such as quercetin, gallic acid, ferulic acid, protocatechuic acid, and kaempferol are found in dried onion peels.[9] Onion peel is considered a waste material that

Received: February 17, 2021
Accepted: June 10, 2021
Published: July 8, 2021

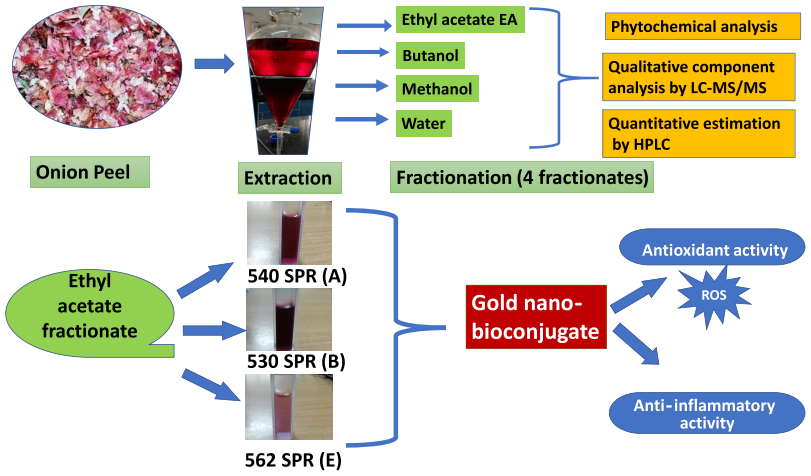

Figure 1. Experimental design of the protocol followed for extracting from onion peel and a further strategy adopted for preparing gold nano-bioconjugates and studying antioxidant and anti-inflammatory activity.

possesses 20 times greater quercetin and quercetin glycosides than the edible part.[12−15] The previous report suggests that the outer layer of red onion possesses the highest antioxidant activities than other varieties of onion as determined by in vitro antioxidant activities[16] and can be used in the treatment of cancer and stress.[17,18]

Reactive oxygen species (ROS) are natural byproducts that are generated as a result of various biochemical reactions, and cell signaling pathways involved in the increased level of ROS are a biomarker of tumor cells and also linked with various diseases such as cancer and cardiovascular and metabolic disorders.[19] The overproduction of ROS has detrimental effects on the cell's structures, functions, and homeostasis and results in oxidative stress.[20] Moreover, an imbalance between the generation of ROS and the detoxification capability of reactive intermediates by the cells causes oxidative stress.[18] Although phytochemicals participated in a major role in reducing oxidative stress by inhibiting the ROS production, however, due to the solubility in water and thermal instability of such phytochemicals, nanotechnology plays an important role in enhancing the bioavailability of plant secondary metabolites due to their high biodegradability, biocompatibility, and slow drug release mechanism.[21−23] Over the past decades, nanotechnology has been extensively used in medicines and has made a huge impact in medicinal sciences.[24−28] This emerging field has wide applications in anticancer, antiviral, anti-HIV, and so on.[29−32] Preparation of gold nanoparticles includes various chemical, physical, and biological methods. In the preparation of gold nanoparticles in addition to chemical and physical methods, the plant extract is used for the preparation of nanoparticles, which is considered the simplest, eco-friendly, and cost-effective approach.[33,34] More recently, green synthesis of metal nanoparticles furnishes the effective utilization of natural compounds in plant extracts, which can act as an excellent reducing agent for the conversion of a metal salt to a nanoparticle.[35−37] Aromal et al. reported the green synthesis of gold nanoparticles by photochemical preparation of seed particles from *Macrotyloma uniflorum*,[38] and another photochemical preparation of seed particles was reported.[39] Another green synthesis of gold and silver nanoparticles from aloe vera plant extract of size 5−50 nm was reported.[40] Researchers have found that the synthesized gold and silver nanoparticles from red algae *Gelidium amansii* possessed potent biological activity against *Escherichia coli*, *Staphylococcus aureus*, and several human pathogens.[41] The ethanolic bark extract of the plant *Terminalia arjuna* was used as a precursor for gold nanoparticle synthesis and exhibited antioxidant, anti-inflammatory, and neuroprotective effects as well as antibacterial, antifungal, and anticancer activities.[42−45] Therefore, the efficacy of the nanotechnology-based approach toward targeted drug delivery to counter inflammation has increased many-fold as compared to the traditional use of medicine.[46]

The current study aimed to synthesize gold nano-bioconjugates from onion peel extract, which is a waste. Onion peel, although a waste, contains many-fold increased quercetin as compared to onion flesh.[47] Instead of using commercially available quercetin as a capping agent for gold nanoparticle synthesis,[48] here, onion peel is used as a cheap source of quercetin, which can act as a strong reducing agent as well as a capping agent, and the synergistic antioxidant and anti-inflammatory activities were also checked. In this work, by giving priority to the sustainable utilization of natural resources, the whole onion peel crude extract was purified into four fractionates, viz., ethyl acetate (EA), butanol, methanol, and water. Different types of antioxidant assays were done on the prepared fractionates. Among them, the ethyl acetate (EA) fractionate showed the highest antioxidant activity. The anti-inflammatory activity was investigated between the pure compound quercetin and the ethyl acetate (EA) fractionate. Furthermore, gold nano-bioconjugates were prepared from the ethyl acetate (EA) fractionate, and their antioxidant and anti-inflammatory activities were examined by comparing with the crude onion peel drug (OPD) to confirm the increased anti-inflammatory activities of gold nano-bioconjugates.

2. RESULTS AND DISCUSSION

Onion peel extract was considered as one of the best antioxidant and anti-inflammatory precursors, as it contains various polyphenols and important flavonoids. Among various flavonoids, quercetin plays an important role in anti-inflammatory activity. Therefore, in this work, onion peel extract was considered as an herbal drug that was further purified into different fractionates such as methanol, butanol,

https://doi.org/10.1021/acsomega.1c00861
ACS Omega 2021, 6, 17811−17823

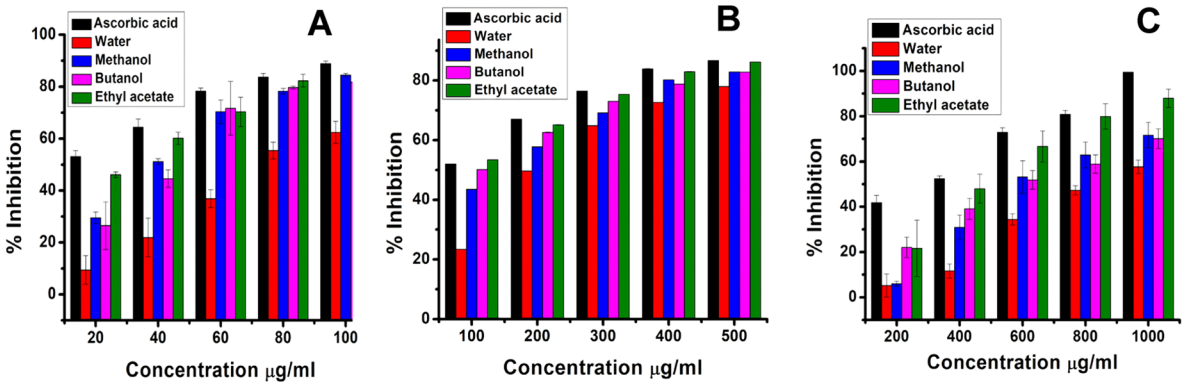

Figure 2. (A) DPPH radical scavenging activity. (B) Reducing power activity. (C) ABTS radical scavenging activity. Data represents the results of experiments done in triplicates, $n = 3$. Values are the mean ± standard deviation of three independent experiments.

ethyl acetate, and water (Figure 1), and the biological activity of each fractionate was investigated.

2.1. In Vitro Antioxidant Assays. *2.1.1. DPPH Radical Scavenging Activity.* In this study, all four fractionates showed concentration-dependent radical scavenging activity against DPPH. Ascorbic acid was considered as a control. At the maximum of 100 μg/mL concentration, ethyl acetate and methanol fractionates showed 84.48% scavenging or inhibition activity, whereas butanol and water showed 81.82 and 62.4% scavenging, respectively. The standard ascorbic acid exhibited 88.81% scavenging with an IC_{50} of 7.8 μg/mL. The IC_{50} values of the ethyl acetate, methanol, water, and butanol fractionates were found to be 22.24, 41.43, 78.35, and 45.17 μg/mL, respectively (Figure 2A). The results are expressed as percentage inhibition of DPPH. The IC_{50} value of ascorbic acid was found to be 7.8 μg/mL.

An earlier report has been found where at 200 μg/mL[49] concentration, DPPH activity of onion waste showed IC_{50} of 83.7, 107.1, 30.1, and 43.7 μg/mL from methanol, distilled water, 70% methanol, and 70% ethanol solvent extraction, respectively. Another report has investigated the DPPH activity of the ethanol fractionate of onion peel, where it showed 72.25 ± 2.74% inhibition at the highest concentration of 200 μg/mL.[50]

From previous reports, it can be concluded that the ethyl acetate fractionates of onion peel waste have shown significant inhibitory activity because the IC_{50} value is very low such as 22.24 μg/mL by keeping the highest concentration of 100 μg/mL.

2.1.2. Reducing Power Activity. In this assay, the reducing power of the extracts was determined by measuring the potentiality of the extracts in reducing Fe^{3+} to Fe^{2+}. The formation of Fe^{2+} results in the change in color from yellow to Prussian blue, and the intensity of color formation is directly proportional to Fe^{2+} formation. A higher reducing power of extracts indicates high antioxidant activity. The optical density (O.D.) of the solutions was taken at 700 nm. At a maximum of 500 μg/mL concentration, the percentage inhibitions of ethyl acetate, butanol, methanol, and water fractionates were found to be 86.18, 82.81, 82.85, and 78.01%, respectively.

Investigations from earlier studies have suggested that the pure compound quercetin showed reducing power activity with an IC_{50} of 50.06 μg/mL.[51] However, it is evident from Figure 2B that the ethyl acetate fractionate showed satisfactory results with an IC_{50} of 28.99 μg/mL, and the reducing power of the fractionates increases with the increase in concentration. The order of reductive potential was ethyl acetate > butanol > methanol > water. The IC_{50} of butanol, methanol, water, and ascorbic acid were obtained to be 60.98, 134, 241.67, and 30.87 μg/mL, respectively, at a maximum of 500 μg/mL concentration.

2.1.3. 2,2′-Azino-bis(3-ethylbenzothiazoline-6-sulfonic acid) Scavenging Activity/ABTS Scavenging Assay. All four fractionates exhibited very significant and efficient $ABTS^{\cdot+}$ radical scavenging activity in a concentration-dependent manner. From the result (Figure 2C), it was found that the order of scavenging effects on $ABTS^{\cdot+}$ was ethyl acetate > butanol > methanol > water. At the highest concentration (1000 μg/mL), ethyl acetate showed the highest activity of 87.95% followed by butanol with 70%, methanol with 71.66%, water with 57.64%, and the standard ascorbic acid with 99.43%. Likewise, the IC_{50} values obtained were 328 μg/mL for ascorbic acid, 468 μg/mL for ethyl acetate, 627.46 μg/mL for butanol, 662 μg/mL for methanol, and 867 μg/mL for water.

2.2. In Vitro Anti-inflammatory Activity. *2.2.1. Inhibition of Bovine Serum Albumin Denaturation.* As the ethyl acetate fractionate showed the highest antioxidant activity as described above in Figure 2A–C, next, we evaluated the anti-inflammatory activity of the ethyl acetate fractionate and compared it with pure quercetin. In the present study, the anti-inflammatory activity was evaluated against bovine serum albumin. Protein denaturation is the major cause of inflammation. The anti-inflammatory activity of the ethyl acetate fraction (EA) was studied, and it showed that inhibition of protein denaturation occurred in a concentration-dependent manner (Figure 3). At the maximum concentration of 1000 μg/mL, the EA fraction showed the highest denaturation inhibition of 74.04%, and the IC_{50} value was found to be 39.92 μg/mL, whereas the pure compound quercetin showed 68.02% inhibition at the same concentration. The IC_{50} value for quercetin was obtained to be 732 μg/mL. Diclofenac sodium was used as a standard anti-inflammatory drug and showed a maximum inhibition of 76.69% at 400 μg/mL. Hence, the data indicate that the ethyl acetate fraction exhibited higher % inhibition than the pure compound quercetin, which demonstrates the effectiveness of the ethyl acetate fractionate as an anti-inflammatory drug. Therefore, the ethyl acetate fractionate of onion peel (OPD) was taken as a model drug in further studies.

2.3. Phytochemical Analysis. *2.3.1. Total Polyphenol and Flavonoid Content.* The total polyphenol and flavonoid

https://doi.org/10.1021/acsomega.1c00861
ACS Omega 2021, 6, 17811−17823

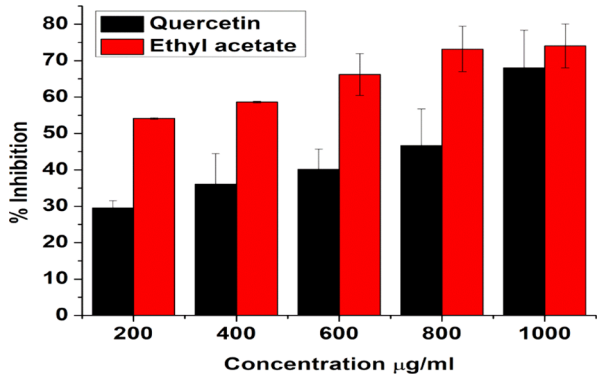

Figure 3. Bovine serum albumin denaturation assay of quercetin and the ethyl acetate fractionate of onion peel extract. Data represents the results of experiments done in triplicates, $n = 3$. Values are the mean ± standard deviation of three independent experiments.

content was determined for all four fractionates and is tabulated in Table 1.

Table 1. The Total Polyphenol (TPC) and Flavonoid (TFC) Content of Four Fractionates

name of fractionates	total polyphenol content (TPC) (mg of GAE/g of extract)	total flavonoid content (TFC) (mg of quercetin/g of extract)
ethyl acetate fractionate	53.44 ± 0.620	43.11 ± 4.55
butanol fractionate	41.67 ± 1.75	23.65 ± 4.92
methanol fractionate	39.72 ± 0.796	37.87 ± 3.71
water fractionate	31.79 ± 1.20	11.41 ± 5.84

Among all four fractionates, ethyl acetate (EA) showed the highest phenolic and flavonoid content. Earlier studies have evaluated the total polyphenol content of red onion and found it to be 4.28 ± 0.28.[52] The TPC contents in the outer layer of violet, white, and green varieties of *Allium cepa* were found to be 43.5, 7.6, and 13.4 mg/g GAE, respectively.[16] Another report shows that the TPC and TFC contents in the dichloromethane fractionate (DCM) are 23.1 ± 0.9 and 1.3 ± 0.4, respectively. Meanwhile, the diethyl ether (DEE) fraction shows 47.3 ± 1.5 TPC and 9.1 ± 1.23 TFC, and the water fractionate shows 27.3 ± 1.7 and 1.5 ± 0.21, respectively.[53]

2.3.2. Identification of Quercetin by LC(ESI)-MS/MS. LC(ESI)-MS/MS analyses were performed to identify the presence of quercetin in the ethyl acetate fractionate of onion peel. Electrospray ionization in positive mode was applied to transfer the analytes from the liquid mobile phase from the HPLC column to the gas phase before introduction into the MS. In ESI positive mode, Figure 4B shows MS/MS data for the selected mother ion for quercetin (m/z 303).

In ESI negative mode, after the loss of glycosyl units, quercetin mono- and diglucosides are predicted to produce quercetin aglycone (m/z 301) (Figure 4A). Surprisingly, peaks produced fragments at both m/z 301 and m/z 303.

The MS/MS data for quercetin fragmentation of the conjugates generates a fragment ion (m/z 303) corresponding to protonated quercetin aglycone, and when further MS/MS fragmentation is performed, it showed the same fragmentation pattern as quercetin. Hence, the ethyl acetate fractionate has a rich content of quercetin.

2.3.3. Quantification of Quercetin in the Ethyl Acetate Fractionate of Onion Peel Extracts. HPLC was also carried out to determine the quercetin content in the ethyl acetate fractionate of onion peel extract. The quercetin content in the ethyl acetate fractionate was found to be 716.5352 μg from 1 mg of the fractionate by plotting the calibration curve, the concentration of quercetin versus peak area. The correlation coefficient of the calibration curve was found to be 0.9975. Figure 5 shows the HPLC chromatogram depicting the peak of the ethyl acetate fraction of onion peel extract produced by a maceration process.

2.4. Characterization of Gold Nano-biocomposites. The ethyl acetate fractionates of onion peel extract (OPD), which was considered as a drug in this work, showed the highest antioxidant activity and were hence successfully utilized in the preparation of gold nano-bioconjugates. Thus, the green extract served as a good reducing agent in the reduction of Au^{3+} to Au^0 and also provided good stability even after one month, thereby increasing the shelf life of the gold nano-bioconjugate. Different concentrations of the ethyl acetate fractionate lead to pink, ruby red, and purple colored solutions of the gold nano-bioconjugate. The colors obtained from gold nano-bioconjugates are due to surface plasmon resonance (SPR). Figure 6A represents the UV−vis spectra of the prepared gold nano-bioconjugates. Furthermore, the result clearly shows distinctive surface plasmon peaks at 530, 540, and 562 nm of three different gold nano-bioconjugates labeled as A, B, and E, respectively. The stability of the gold nano-bioconjugate was found to be good at least for one month, which was also determined by UV−vis spectroscopy. The detailed morphology of the gold nano-bioconjugate was evaluated by using transmission electron microscopy (TEM). Figure 6B shows a representative TEM image of prepared gold nano-bioconjugates. It is clear from the image that the gold nanoparticles formed are spherical, fairly dispersed having sizes below 20 nm. Fourier transform infrared spectroscopy (FTIR) was also carried out with gold nano-bioconjugate B.

The FTIR spectrum shows a strong peak at 3420 cm^{-1} due to $O-H_{str}$ primarily due to alcohol OH from quercetin and other alcohol moieties stabilizing the gold nanoparticles. Other notable peaks at 1630, 2924, and 2850 cm^{-1} are due to the presence of C═O, $C-H_{str}$, and C−H, respectively. The peak at 1387 cm^{-1} can be due to the CH_3 bend. Peaks at 1280 and 1166 cm^{-1} are due to C−O−C and $C-OH_{str}$, respectively.

2.5. In Vitro Antioxidant Activities of Gold Nano-bioconjugates. *2.5.1. DPPH Radical Scavenging Activity.* The unpaired electrons of free radicals constantly tend to form a stable bond, either by gaining or losing an unpaired electron. The presence of an excessive amount of such free radicals always leads to severe damage or mutation to DNAs resulting in permanent damage to the cells.[54] Bimetallic nanoparticles (BNPs) such as Ag−Cu and Ag−Zn BNPs synthesized from the medicinal plant *Annona muricata* shows DPPH radical scavenging activity with IC_{50} of 75.08 and ≥100 μg/mL.[55] Similarly, AuNPs from *Ziziphus nummularia* leaf extract show DPPH scavenging with an IC_{50} of 520 μg/mL.[56] Another study has evaluated the IC_{50} of zinc oxide nanoparticles (ZnONPs) prepared from *Alhagi maurorum* leaf aqueous extract to be 125 μg/mL.[57] However, in this study (Figure 7A), the highest DPPH radical scavenging activity was shown by B, 87.42%, followed by A, 83.44%, OPD, 83.58%, and E, 70.98%, with

https://doi.org/10.1021/acsomega.1c00861
ACS Omega 2021, 6, 17811−17823

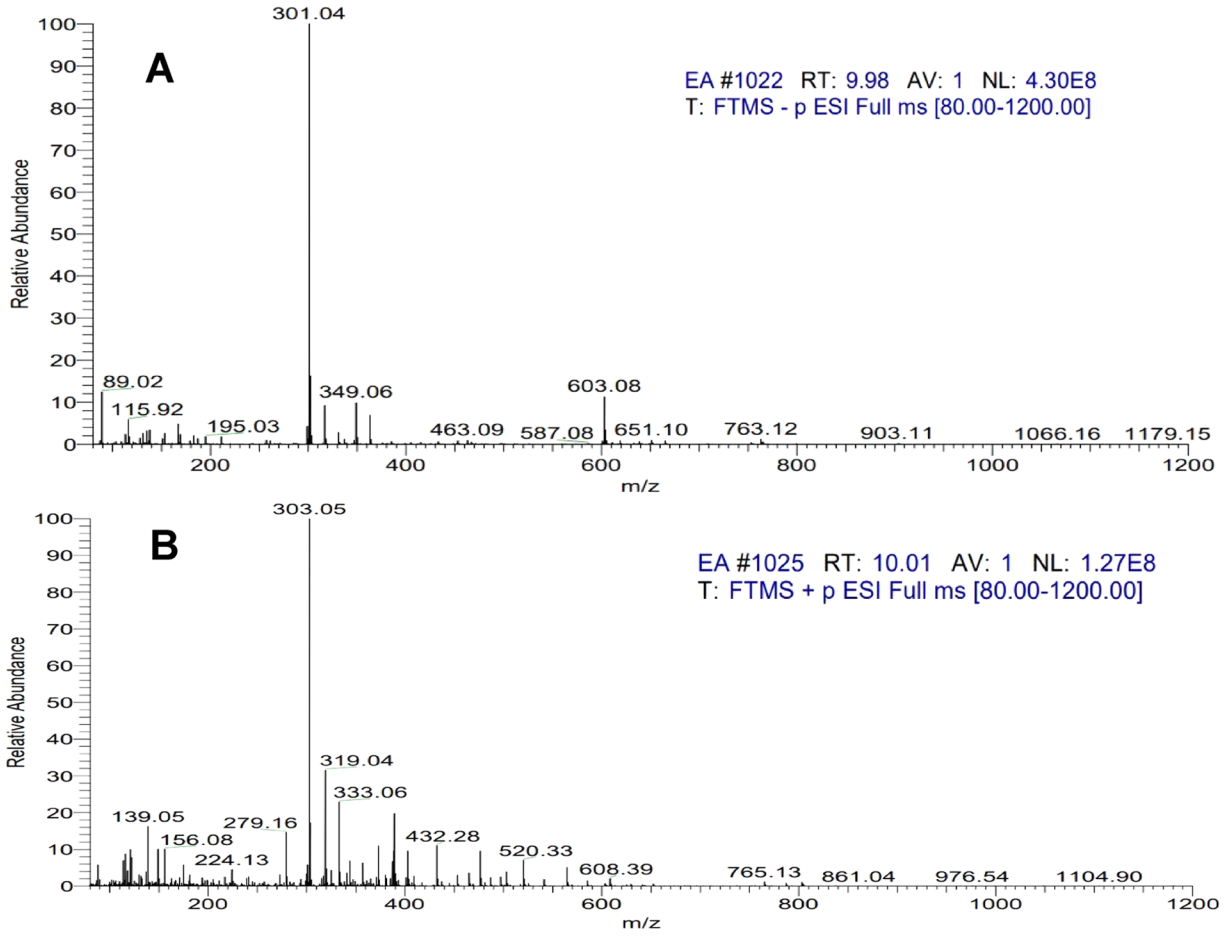

Figure 4. (A) LC(ESI)-MS/MS negative mode spectra of quercetin identified in the ethyl acetate fraction of onion peel extract peaks identified in the HPLC chromatogram and (B) LC(ESI)-MS/MS positive mode spectra.

IC_{50} values of 28.92, 30.48, 34.80, and 56.66 μg/mL, respectively. All three gold nano-bioconjugates showed concentration-dependent radical scavenging activity against DPPH. The results are expressed as percentage inhibition of DPPH. Here, gold nano-bioconjugate B can act as a potent antioxidative agent by readily accepting or donating electrons or protons to free radicals thereby promoting the formation of stable bonds. The standard ascorbic acid exhibited 90.27% percentage inhibition with an IC_{50} value of 29.45 μg/mL, which is comparable with gold nano-bioconjugate B.

2.5.2. Reducing Power Activity. In this assay, the reducing power of the extracts was determined by measuring the potentiality of the extracts in reducing Fe^{3+} to Fe^{2+}. The formation of Fe^{2+} results in the change in color from yellow to Prussian blue, and the intensity of color formation is directly proportional to Fe^{2+} formation. A higher reducing power of extracts indicates high antioxidant activity. The optical density (O.D.) of the solutions has been taken at 700 nm. Figure 7B demonstrates that the reducing power of the gold nano-bioconjugates increases with an increase in concentration. The highest reducing power activity shown by B is 81.25% at a maximum of 100 μg/mL concentration followed by A and OPD and then E with 79.68 and 77.63%, respectively. The IC_{50} values of B, A, E, and OPD are as follows 38.56, 42.19, 44.84, and 47.23 μg/mL, respectively. On the other hand, the Ag nanoparticles synthesized from dragon tongue bean peels (DtbP-AgNPs) possessed an IC_{50} value of 88.37 μg/mL[58] as compared to gold nano-bioconjugate B with 38.56 μg/mL, which indicated that B can act as an efficient antioxidant agent. Ascorbic acid served as a standard and exhibited 83.61% inhibition, which is comparable with gold nano-bioconjugate B with 81.25% inhibition.

2.5.3. ABTS Scavenging Activity. The gold nano-bioconjugates exhibited very significant and efficient $ABTS^{\cdot+}$ radical scavenging activity in a concentration-dependent manner. At a maximum of 100 μg/mL concentration, B possessed the highest activity of 98.34% followed by A, OPD, and E with 98.29, 92.91, and 79.72%, respectively. However, the IC_{50} value of gold nanoparticles from *Ziziphus nummularia* leaf extract was found to be 690 μg/mL.[56] Meanwhile, the gold nano-bioconjugate B showed 50.28 μg/mL. It is evident from Figure 7C that the order of scavenging effects of extracts on $ABTS^{\cdot+}$ is B > A > OPD > E with IC_{50} values of 50.28, 53.87, 55.77, and 70.28 μg/mL, respectively, and the standard ascorbic acid shows 99% inhibition with a 32.21 μg/mL IC_{50}.

2.6. MTT Assay. Finally, for efficient anti-inflammatory drug delivery, it is important to check the toxicity of the gold nano-bioconjugate in the living system. Therefore, the viability of the cell has been evaluated from an MTT assay performed for 24 h in the L6 muscle cell line. Here, three nano-bioconjugates (A, B, and E) were tested at different concentrations (10, 50, 100, and 200 μg/mL). The cell viability experiment showed the non-cytotoxicity nature of gold nano-bioconjugates. Among the three nano-bioconjugates, A showed the highest cell viability (100%) at 10 μg/mL concentration. However, as the concentration increases to 200

https://doi.org/10.1021/acsomega.1c00861
ACS Omega 2021, 6, 17811−17823

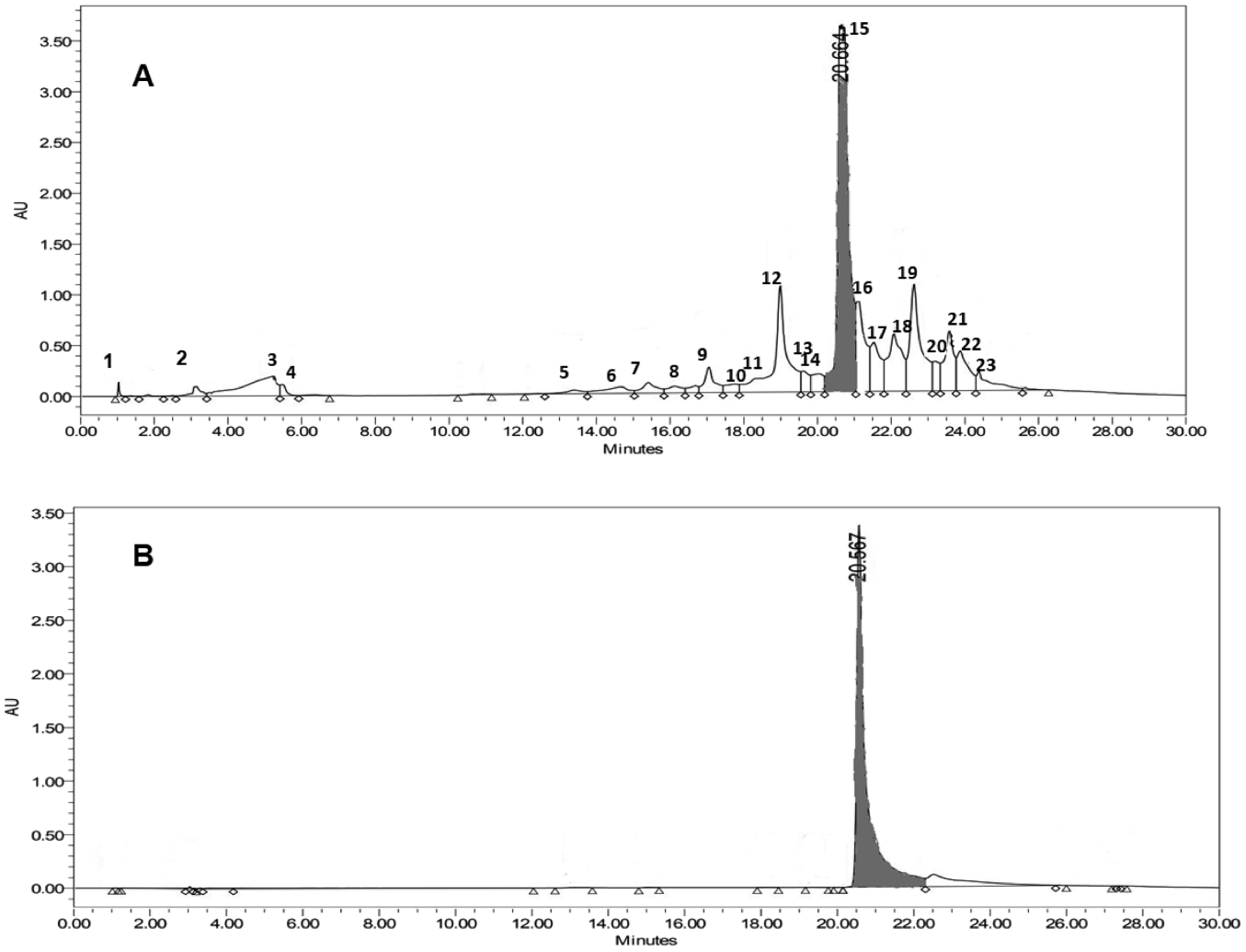

Figure 5. HPLC chromatogram of the ethyl acetate fraction of onion peel extract. (A) Ethyl acetate fraction. (B) Standard quercetin.

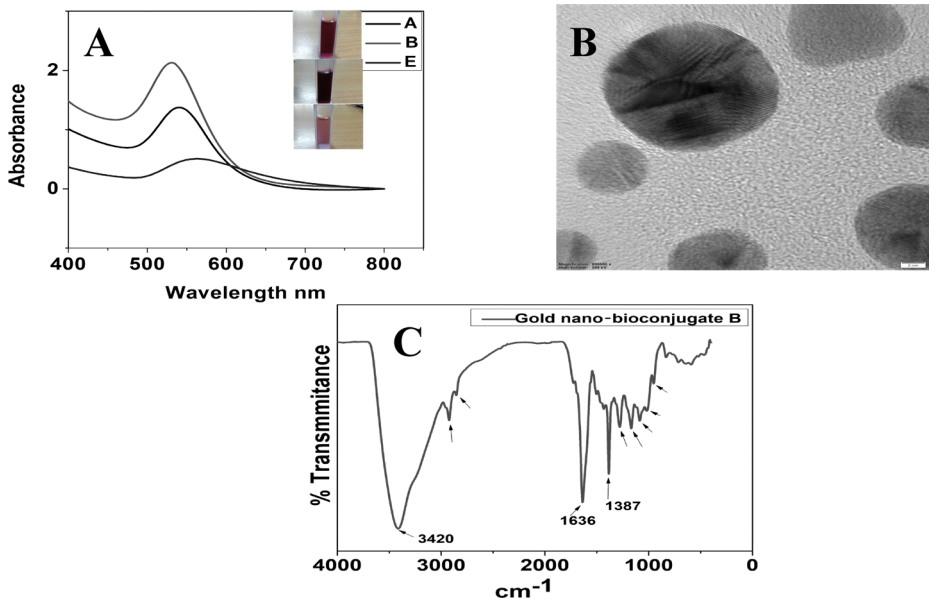

Figure 6. (A) Stacked UV−vis spectra of three gold nano-bioconjugates prepared using different concentrations of onion peel extract. (inset) Colors of the gold nano-bioconjugates. (B) Representative transmission electron microscope (TEM) image. (C) FTIR spectrum of a gold nano-bioconjugate prepared using onion peel extract.

https://doi.org/10.1021/acsomega.1c00861
ACS Omega 2021, 6, 17811−17823

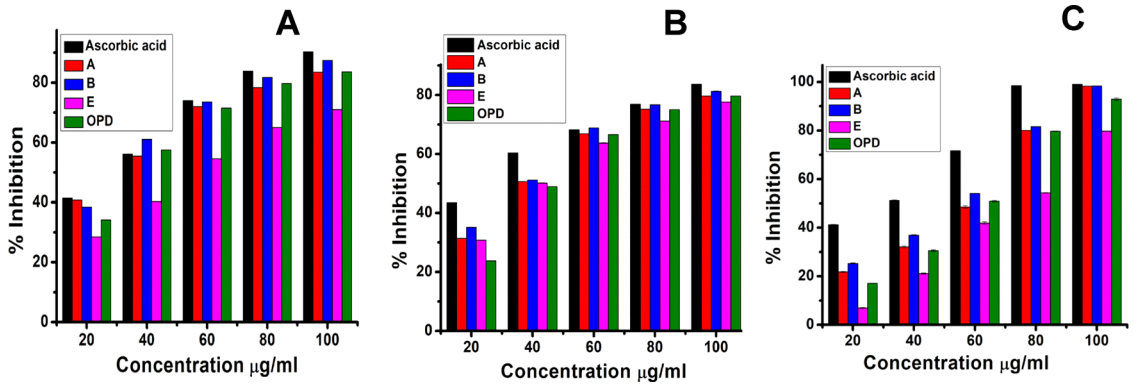

Figure 7. (A) DPPH radical scavenging activity. (B) Reducing power activity. (C) ABTS radical scavenging activity. Data represents the results of experiments done in triplicates, $n = 3$. Values are the mean ± standard deviation of three independent experiments.

µg/mL, the viability of the cell slightly decreases to 73.07%. Meanwhile, gold nano-bioconjugate B showed 86.88% cell viability at 10 µg/mL and 72.3% at 200 µg/mL. Likewise, gold nano-bioconjugate E showed 90.95% at 10 µg/mL and 69.15% at 200 µg/mL. In comparison, OPD showed 99.01% viability at 10 µg/mL and 88.56% at 200 µg/mL concentration (Figure 8). From the results of the cell viability test, it is confirmed that

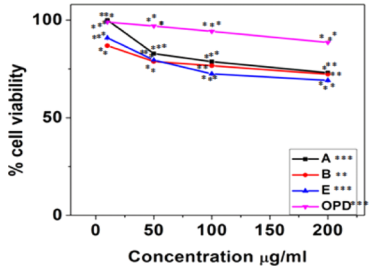

Figure 8. MTT assay in the L6 cell line study with three gold nano-bioconjugates A, B, and E. Data represents the results of experiments done in triplicates, $n = 3$. Values are the mean ± standard deviation of three independent experiments. The statistical significance of the difference between treated and control groups was analyzed using one-way ANOVA followed by all pairwise multiple comparison procedures (Student−Newman−Keuls method). An asterisk (*) represents a significance difference when compared to control values at $*p < 0.05$ ($*p < 0.05$; $**p < 0.01$; $***p < 0.001$).

all three nano-bioconjugates do not show marked cytotoxicity. This indicates that the use of these gold nano-bioconjugates (A, B, and E) is biocompatible and safe for drug delivery in in vitro cell assays.

2.7. Cellular Antioxidant Activity (CAA). *2.7.1. ROS Assay.* The ROS assay was performed to investigate the effect of gold nano-bioconjugates in the intracellular production of ROS, where it was found that the production of ROS decreases with the increase in the concentrations of A, B, E, and OPD compared to the untreated control. Among the four treatments of gold nano-bioconjugates, B showed a significant decrease in ROS generation (Figure 9) with the increase in the concentration. At the minimum of 10 µg/mL concentration, 49.88% ROS reduction was observed. This reduction gradually increased and reached up to 76.77% at a maximum concentration of 200 µg/mL. The reduction of ROS was also shown by OPD with 68.17% from the untreated control at a higher dose of 200 µg/mL, which is less than that of gold nano-bioconjugate B. Meanwhile, gold nano-bioconjugates A

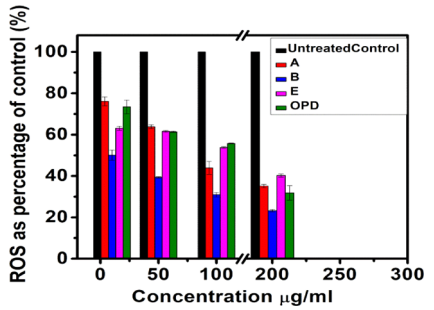

Figure 9. ROS scavenging assay in the L6 cell line. Data represents the results of experiments done in triplicates, $n = 3$. Values are the mean ± standard deviation of three independent experiments.

and E show 64.85 and 59.75% at a maximum dose of 200 µg/mL. The high reduction of ROS by B may be due to the higher load of the ethyl acetate fractionate of onion peel. Thus, gold nano-bioconjugate B showed elevated antioxidant activity and was able to protect the cells from oxidative stress in comparison with the OPD alone. This study indicated that the use of nano-bioconjugates has some additional advantages over the single use of a traditional phytochemical agent.

2.8. In Vitro Anti-inflammatory Activity. *2.8.1. Inhibition of Bovine Serum Albumin Denaturation. 2.8.1.1. Mechanistic Insight into Inhibition of Inflammation.* The defensive mechanism of inflammation involves the vigorous release of lysosomal enzymes, e.g., proteinases lead to promote tissue damage, which results in further inflammation.[59] A report has been found from the previous study that onion peel has an impact on the gene expression that is associated with inflammation. Lipopolysaccharides (LPS) simulated in an HT-29 cell model showed downregulation of TNF-α mRNA expression in HT cells (OPE-treated) as compared with the control (LPS simulated non-treated), whereas a marked increase in the expression of HO-1 (heme oxygenase-1) and GSTs (glutathione *S*-transferase) has been found after the treatment of LPS.[60]

Semecarpus anacardium bark[61] and various plant species such as an ethanolic extract of *Wedelia trilobata*[62] showed the inhibition of protein denaturation activity by using BSA. Since protein denaturation is a feature of inflammation, therefore the plant extract showed anti-inflammatory activity by preventing the thermal instability of proteins. The actual mechanism behind the stability of the membrane is yet to be investigated. Proteinase inhibitors play an important role in the protection

https://doi.org/10.1021/acsomega.1c00861
ACS Omega 2021, 6, 17811−17823

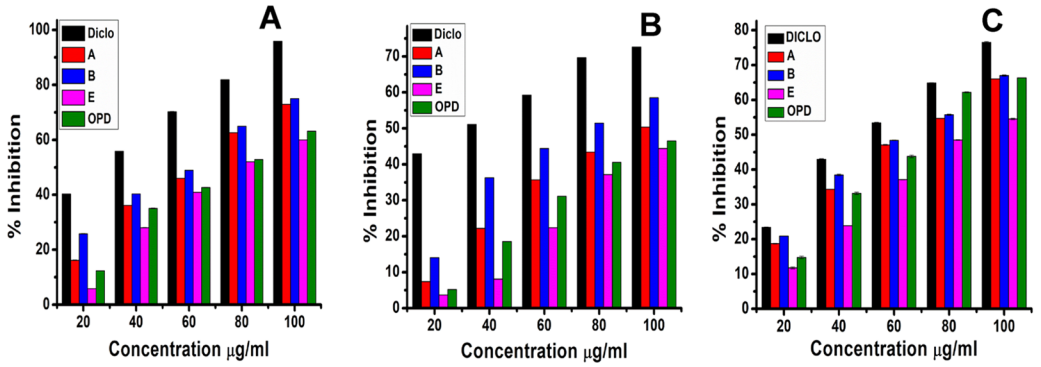

Figure 10. (A) BSA inhibition test. (B) Proteinase inhibition test. (C) Lipoxygenase inhibition assay of three gold nano-bioconjugates A, B, and E. Data represents the results of experiments done in triplicates, $n = 3$. Values are the mean ± standard deviation of three independent experiments.

of membranes. The presence of flavonoids in plants has strong antioxidant and anti-inflammatory activities; thereby, at the site of inflammation, such a high flavonoid content might hinder the lysosomal matter of neutrophil release.[62] However, in vitro and in vivo studies are needed to know the actual mechanism of inhibition of inflammation and also to check the acute toxicity of nano-bioconjugates in vivo.

Here, gold nano-bioconjugates exhibiting their capacity to inhibit protein denaturation might become good anticipation for utilization of drug development in treating inflammation. The activity of gold nano-bioconjugates was mentioned as the IC_{50} value, which indicates the concentration required to inhibit the protein denaturation by 50%. Just as the in vitro anti-inflammatory activity was evaluated against bovine serum albumin for the ethyl acetate onion peel extract fraction, which showed excellent inhibition of protein denaturation occurring in a concentration-dependent manner, similarly, in vitro anti-inflammatory activity was evaluated against bovine serum albumin for gold nano-bioconjugates. To investigate the anti-inflammatory activity among the three nano-bioconjugates and the ethyl acetate fractionate of onion peel (OPD), a BSA test was carried out. Figure 10A shows that gold nano-bioconjugates A, B, and E exhibited anti-inflammatory activity at 100 μg/mL concentration (maximum concentration) with 72.92, 75.06, and 60% percentage inhibitions, respectively. The IC_{50} values determined for A, B, and E were 64.58, 58.31, and 79.07 μg/mL, respectively. The standard drug diclofenac sodium exhibited 95.84% activity at the highest concentration of 100 μg/mL with an IC_{50} of 32.53 μg/mL. Likewise, the fractionate OPD showed 63.18% inhibition activity with an IC_{50} of 74.69 μg/mL, which indicated that the OPD activity is significantly less than the gold nano-bioconjugate B. A phytoassisted synthesis of magnesium oxide (MgO-NPs) nanoparticles from *Pterocarpus marsupium* Roxb. heartwood extract has shown a protein inhibition of 16.26% at a minimum of 20 μg/mL concentration and 56.53% denaturation inhibition at a maximum of 100 μg/mL concentration with an IC_{50} of 81.69 μg/mL.[54] Meanwhile, nano-bioconjugate B showed 25.84% denaturation inhibition at the lowest concentration of 20 μg/mL and 75.06% at the highest concentration of 100 μg/mL, and the IC_{50} was found to be 58.31 μg/mL, which shows significant inhibitory activity in denaturation of proteins. However, among all three nano-bioconjugates, B showing the highest anti-inflammatory activity may be due to the higher concentration of the ethyl acetate fractionate onto the surface of the nanoparticles. On the contrary, among all three nano-bioconjugates, E showed the least activity.

2.8.2. Proteinase Inhibition Test. The basic principle of the proteinase inhibition test involves inflammation in the process of development of tissue damage, and the leukocyte's proteinase plays an important role. Remarkable protection was provided by proteinase inhibitors.[63] Here, the standard diclofenac showed 72.59% inhibition with an IC_{50} of 36.57 μg/mL at a maximum concentration of 100 μg/mL. A study suggested that ethyl acetate extract of the leaves and flowers of *Mikania micrantha* exhibited 1180 and 1250 μg/mL IC_{50}, respectively.[64] Among the three different concentrations, gold nano-bioconjugate B showed the highest anti-inflammatory activity of 58.51% at 100 μg/mL with an IC_{50} of 77.36 μg/mL, whereas OPD, A, and E showed 46.51, 50.37, and 44.44% at 100 μg/mL (Figure 7B). From the results, it can be concluded that B possessed good anti-inflammatory activity as compared to the OPD. Meanwhile, E shows less activity, which is more or less equivalent to OPD. This also indicates that the preparation of gold nano-bioconjugates by the addition of a high amount of the ethyl acetate fractionate increases the efficacy of drug release as compared to the single use of the EA fraction of OPD.

2.8.3. Antilipoxygenase Assay. The plant lipoxygenase pathway is in many aspects equivalent to the "arachidonic acid cascades" in animals.[65] For this reason, the in vitro inhibition of lipoxygenase (LOX) constitutes a good model for the screening of plants with anti-inflammatory potential.[66] LOXs are sensitive to antioxidants, and most of their action may consist of inhibition of lipid hydroperoxide formation due to scavenging of lipid peroxyl radicals formed in the course of enzyme peroxidation. From one study, it has been shown that ethyl acetate extract of the leaves and flowers of *Mikania micrantha* exhibited 98 and 185 μg/mL IC_{50}, respectively.[64] Meanwhile, gold nano-bioconjugate B showed a 67.12 μg/mL IC_{50}. At 100 μg/mL concentration, the percentage inhibitions shown by gold nano-bioconjugates B, A, E, and OPD were 66.99, 66.01, 66.33, and 54.52%, respectively. The IC_{50} of all three gold nano-bioconjugates (A, B, and E) were found to be 70.13, 67.12, and 86.94 μg/mL, respectively. However, the IC_{50} of OPD obtained was 69.01 μg/mL. Likewise, diclofenac sodium (DICLO), which was taken as a model anti-inflammatory drug, showed a 56.54 μg/mL IC_{50} and 76.5% inhibition. From this result, it can be concluded that among all three gold nano-bioconjugates, B showed good antilipoxygenase activity.

https://doi.org/10.1021/acsomega.1c00861
ACS Omega 2021, 6, 17811−17823

3. CONCLUSIONS

In this work, we have reported the green synthesis of gold nano-bioconjugates from the ethyl acetate (EA) fraction of onion peel for the first time, which is cost-effective and eco-friendly. Here, preparation of gold nano-bioconjugates by using cheap biowaste without the involvement of any additional chemicals could be an alternative approach for metal nanoparticle synthesis, which synergistically shows good antioxidant and anti-inflammatory activity. The antioxidant activity of the ethyl acetate fractionate was found to be the highest among all other four fractionates. These bioactive components were identified, and a high amount of quercetin is found to be present as confirmed by LC-MS/MS and HPLC. The ethyl acetate fractionate possessed strong anti-inflammatory activity as compared with pure quercetin. The fractionate contains mixed flavonoids or polyphenols, which enhances the anti-inflammatory activity by the mode of synergistic action. The total flavonoid and phenol contents in the ethyl acetate fractionate also indicate the direct relation with antioxidant activities. An increase in the total polyphenol content (TPC) and total flavonoid content (TFC) increases the antioxidant activities, which in turn increases the anti-inflammatory activity. Preparation of gold nano-bioconjugates with different ethyl acetate fractions (A, B, and E) also showed good antioxidant and anti-inflammatory activity as compared with the OPD (onion peel drug) alone. Among the three gold nano-bioconjugates, B showed good antioxidant and anti-inflammatory activity, which also indicates that the loading of a high concentration of the ethyl acetate fractionate is directly proportional to inhibition of inflammatory activity. The synthesized gold nano-bioconjugates act as an additive, where the biowaste product onion peel played the role of a potent reducing agent as well as possessed good antioxidant activity.

This work emphasizes the development of an economical, one-step, and environment-friendly nano-bioconjugate from cheap biowaste sources, which can be utilized as an effective antioxidant and anti-inflammatory agent. Furthermore, cell-based assays are needed to understand the mechanism and actual effects in in vivo experiments. However, an active component of the ethyl acetate fractionate is required to be extracted, and an investigation to explore the actual mechanism of action is needed.

4. MATERIALS AND METHODS

4.1. Reagents. 1,1-Diphenyl-2-picrylhydrazyl (DPPH), ascorbic acid (AA), quercetin, BSA, casein, and lipoxygenase were obtained from Sigma-Aldrich, linoleic acid was from SRL, gold(III) chloride trihydrate ($HAuCl_4 \cdot 3H_2O$) was from Himedia, and all the remaining chemicals used in this study were of analytical grade and purchased from Merck, Germany.

4.2. Plant Materials. The red onion (*Allium cepa*) peels were collected from a local marketplace in Garchuk, Guwahati, Kamrup district of Assam, India, in the months from April to June. The peels were washed under running water and dried under sunlight for 5 days until moisture was completely removed. Dried onion peels were then powdered using a blender and stored at 4 °C for further use.

4.3. Preparation of Onion Peel Extracts. The dried onion peel extract (228.36 g) was dissolved in methanol at a 1:20 (w/v) ratio for 72 h with gentle shaking in a shaker for 4 h by the maceration process. After filtration through Whatman filter paper, the solid residue was re-extracted twice with the above-mentioned procedure. The extract was then collected and concentrated under reduced pressure and vacuum-dried by a rotary evaporator at 45 °C. The dried extract was then weighed and stored at 4 °C before analysis. Preservatives were not added. The resultant yield of dried methanolic extract was 205 g. Methanolic extract (10 mg) was subjected to thin-layer chromatography and examined in a solvent system of butanol/acetic acid/water (5:1:4). Ten grams of the extract is then separated by a solvent extraction method with ethyl acetate/water (7:3) and water/butanol (4:8). All fractions were then collected, dried, and stored in airtight containers at −20 °C until use. For further biological assays, fractionates were kept preservative-free.

4.4. Phytochemical Analysis. *4.4.1. Total Polyphenol Content.* Total phenolic contents of all the four extracts were determined using the Folin and Ciocalteu reagent using the method[62] with slight modifications. All the four extracts (0.5 mL) were mixed with the Folin and Ciocalteu reagent (2.5 mL, diluted 10 times) and incubated for 2 min at room temperature followed by the addition of sodium carbonate solution (2 mL, 7.5% w/v). The mixture was then allowed to stand for 30 min at room temperature, and absorbance was measured at 765 nm. The amount of total polyphenol was calculated as a gallic acid equivalent from the calibration curve of the standard gallic acid solution and expressed as mg GAE/g of extract.

4.4.2. Total Flavonoid Content. The total flavonoid content was determined by the method[54] with slight modification. Two milliliters of each extract of methanol, water, butanol, and ethyl acetate was mixed with 2 mL of $AlCl_3$ in methanol (2%). Absorbance was measured at 415 nm after 10 min. Quercetin was used as a reference compound, and the result was expressed as mg of quercetin equivalents (QE)/g of extract.

4.5. Qualitative Component Analysis by LC(ESI)-MS/MS Analysis. Chromatographic separation was carried out using a UHPLC system coupled with a triple quadrupole Orbitrap MS/MS. It consists of an UltiMate 3000 rapid separation LC (Dionex, Inc., Sunnyvale, CA, USA) equipped with a binary pump, a degasser, an autosampler, a thermostated column compartment, a control module, and a Thermo Exactive plus Orbitrap triple quadrupole mass spectrometer (Thermo Scientific) equipped with an electrospray ionization (ESI) interface. Chromatographic separation was performed on a Hypersil Gold C18 column (1.9) operated at 25 °C. Gradient chromatographic separation was performed for an extract of the samples using a mobile phase of solvent A: water and solvent B: methanol, with a constant flow rate of 0.2 mL/min. Samples (10 μL) were injected using an RS-3000 autosampler (Dionex, Inc., Sunnyvale, CA, USA) onto a Hypersil Gold C18 column (150 × 3.00 mm, Thermo, USA). The rapid screening run time of 10 min started with the gradient program of 95% A for 2 min followed by the linear gradients from 5% B to 95% B from 2 to 8 min, held at 95% B for 1 min, and returned to the initial conditions (5% B) in 1 min and re-equilibration of the column. The PDA detector was used to record the chromatogram. Mass spectra were recorded within 10 min. The injection volume and the flow rate were set to 10 μL and 200 μL/min, respectively.

Xcalibur software was used for data acquisition and processing. The full-screen mass spectra from m/z 200 to 2000 mAU were acquired in both modes and with an automatic gain control (AGC) target of 1e6, with a resolution of 35,000. Operation parameters were as follows: source spray

https://doi.org/10.1021/acsomega.1c00861
ACS Omega 2021, 6, 17811−17823

voltage, 4.20 kV; sheath gas flow rate, 25 arbitrary units; auxiliary gas flow rate, 6 arbitrary units; sweep gas flow rate, 2 arbitrary units; spray current, 0.80−1.00; capillary temperature, 270 °C.

4.6. Determination of Phenolic Compounds: HPLC Analysis. HPLC was performed at 25 ± 1 °C using the ethyl acetate fraction of onion peel, which was dissolved in HPLC-grade methanol (10 mg/mL) and filtered through membrane filters (0.45 μm pore size), and a 20 μL volume was injected into the HPLC instrument. The flow rate was maintained at 1 mL/min. The sample was analyzed using a Shimadzu system (Kyoto, Japan) equipped with an LC-20AT Prominence liquid chromatography pump, a DGU-20A3 Prominence degasser, a CBM-20A Prominence communication bus module, an SPD-20A Prominence UV/VIS detector, LC solution software, and a Rheodyne injector with a 100 μL loop. Separation was achieved using a Phenomenex RP C18 column, 250 × 4.6 mm, 5 μm; gradient elution with a gradient mobile phase was performed with solution A (50 mM sodium phosphate in 10% methanol; pH 3.3) and solution B (70% methanol) in the following gradient elution program: 0−15 min, 100% solution A; 15−45 min, 70% solution A; 45−65 min, 65% solution A; 65−70 min, 60% solution A; 70−95 min, 50% solution A; 95−100 min, 0% solution with a flow rate of 1 mL/min. The peaks were identified using UV absorbance at 254 nm, and quercetin was used as a standard flavonoid.

4.7. Antioxidant Assay. *4.7.1. DPPH Radical Scavenging Assay.* The DPPH (1,1-diphenyl-2-picrylhydrazyl) radical scavenging activities of methanol, ethyl acetate, butanol, and water or aqueous fractionates were determined by a standard method.[55] The extract was diluted in methanol and made 20, 40, 60, 80, and 100 μg/mL dilutions. Briefly, 100 μL of 0.2 mM DPPH in methanol solution was added to 50 μL of sample solution to each of 96-well plates. The reaction mixture was mixed thoroughly and incubated in the dark for 30 min. Absorbance was measured at 517 nm using a UV−vis spectrophotometer. Methanol was kept in control. Each experiment was performed in triplicates.

The percentage of radical scavenging activity of DPPH by the extracts was calculated by the following formula

$$\text{Percentage DPPH radical scavenging scavenging} = [(\text{Ac} - \text{At})/\text{Ac}] \times 100$$

where Ac = absorbance of the control and At = absorbance of the test sample.

4.7.2. Reducing Power Activity. The reducing power assay of four fractionates was performed by ferric reducing power assay[62] with slight modification. Briefly, 0.2 mL volumes of different concentrations of 100, 200, 300, 400, and 500 μg/mL sample extracts were mixed with 2.5 mL of 0.2 M phosphate buffer at pH 6.6 and 2.5 mL of 1% potassium ferricyanide. The reaction mixture was incubated at 50 °C for 20 min, 2.5 mL of trichloroacetic acid (10%) was added, and each reaction mixture was centrifuged at 10,000 rpm for 5 min. Then, 2.5 mL of the supernatant was collected and mixed with 2.5 mL of water and 0.5 mL of ferric chloride (0.1%). Absorbance was measured at 700 nm using a UV−vis spectrophotometer. The increased absorbance of the reaction mixture indicated greater reducing power. Each experiment was performed in triplicates at each concentration.

4.7.3. ABTS Radical Scavenging Assay. ABTS was dissolved in water to a 7 mM concentration. ABTS radical cations were produced by reacting ABTS stock solution with 2.45 mM potassium persulfate. The mixture was kept in the dark at room temperature for 16 h before use. The solution was diluted in ethanol (about 1:88 v/v) to give an absorbance of 0.700 ± 0.02 at 734 nm before doing an assay. Fifty microliter volumes of different concentrations of 200, 400, 600, 800, and 1000 μg/mL sample extracts were mixed with 100 μL of ABTS and incubated at room temperature for 30 min.

Based on the results of various antioxidant assays, the fraction that had the highest antioxidant potential was further checked for anti-inflammatory activity. Bovine serum denaturation inhibition assay was carried out to test the anti-inflammatory activity.

4.8. In Vitro Anti-inflammatory Assay. Bovine serum denaturation inhibition assay is one such assay to detect the preliminary anti-inflammatory activity. The assay was conducted with the ethyl acetate fraction of onion peel, which had the highest antioxidant potential, to check its ability to inhibit the denaturation of BSA. A comparison was done between the pure compound quercetin and the ethyl acetate fraction.

4.8.1. BSA Denaturation Inhibition Assay. Inhibition of albumin denaturation was checked by the standard method[62] with slight modification. Different concentrations of four fractions, ethyl acetate (EA), butanol, methanol, and water fractionates, were made (200, 400, 600, 800, and 1000 μg/mL) and added to 1.8 mL of 1% BSA solution. The pH was adjusted to 6.5 using 1 N HCl, and the solution was incubated at 37 °C for 20 min and then heated to 57 °C for 10 min. After cooling, turbidity was measured using a UV−vis spectrophotometer at a 660 nm absorbance. Diclofenac sodium was used as the standard, and a solution without a sample/extract was considered as the control. The experiment was done in duplicates. The relative percentage inhibition of protein denaturation was calculated.

$$\%\text{Inhibition} = (\text{Abs control} - \text{Abs sample}) \times 100/\text{Abs control}$$

4.9. Synthesis of Onion Peel (OPD)-Loaded Gold Nanoparticles. Briefly, three different concentrations of the ethyl acetate fractionate (EA) of the OPD, that is, 1 mL, 2 mL, and 500 μL, were added in 10 mL of 1 mM gold chloride solution with different time durations: 25, 10, and 30 min, respectively. The whole solution was vigorously stirred on a magnetic stir plate at 33 °C for the respective periods until there is a color change. The three solutions obtained pink (A), ruby red (B), and purple (E) colored solutions, respectively. The solutions were kept at 4 °C for further biological assays. The gold nanocomposites were stable for at least 1 month.

4.10. Characterization of Gold Nano-biocomposites. UV−vis spectra of the three gold nanocomposites (A, B, and E) were recorded using a Shimadzu UV 2600 UV−vis spectrophotometer. The morphology of nanoparticles was examined using a TEM JEOL 2100 plus instrument. Fourier transform infrared spectroscopy (FTIR) analysis was carried out on a PerkinElmer instrument.

4.11. Cell Culture. L6 myoblast cells (rat skeletal muscle) were procured from the National Centre for Cell Sciences (NCCS), Pune, India. Cells were cultured and maintained in Dulbecco's modified Eagle's medium (DMEM) (4.5 g/L) with 10% heat-inactivated fetal bovine serum (FBS), 1% antibiotic−antimycotic, cultured in a T-75 cm^2 flask, and kept at 37 °C in

https://doi.org/10.1021/acsomega.1c00861
ACS Omega 2021, 6, 17811−17823

an incubator with 5% atmospheric CO_2 and observed daily at an inverted microscope Leica DMi1.

4.12. Cell Viability Assay: MTT Assay. Cells were seeded in 96-well plates (1×10^5 per well) with a growth medium of 200 μL and incubated for 24 h. After the incubation for 24 h, treatments using three different gold nanocomposites (A, B, and E) and the onion peel drug (OPD) were done with varying concentrations (10, 50, 100, and 200 μg/mL). The experiment was done in triplicate. After 24 h of drug treatment, cells were washed with phosphate-buffered saline (PBS), old media were replaced with fresh media, and 20 μL of 3-(4,5-dimethylthiazol-2-yl)-2,5-diphenyl tetrazolium bromide (MTT) was added to check cell viability. Cells were incubated for 4 h, which is followed by the addition of 100 μL of DMSO, left for 2 h in the dark. Absorbance was measured at 570 nm using a microplate reader. Non-treated cells were considered as the control. The percentage of cell viability was calculated by the following formula

$$\text{Cell viability\%} = (\text{Abs sample} - \text{Abs blank}/\text{Abs control} - \text{Abs blank}) \times 100$$

4.13. ROS Scavenging Assay. ROS scavenging assay is a cell-based assay that measures the reactive oxygen species such as hydroxyl and peroxyl generated within the cells. The fluorogenic probe (DCF-DA) 2′7′-dichlorodihydrofluorescein is a cell-permeable dye that is deacetylated by cellular esterases to a non-fluorescent compound, which is later oxidized by intracellular ROS to the highly fluorescent 2′,7′-dichlorofluorescein (DCF). Cells were seeded in 96-well plates with a density of 5×10^4 cells per well overnight. After that, cells were treated with different concentrations (10, 50, 100, and 200 μg/mL) of gold nano-bioconjugates (A, B, and E) and the OPD for 24 h. Then, 100 μM TBHP (*tert*-butyl hydroperoxide) was used to treat the cells for 2 h. Cells untreated with 100 μM TBHP were kept as a positive control. After that, cells were washed with 1× PBS two times, and 100 μM DCF-DA was added in cells and incubated for 30 min at a 37 °C CO_2 incubator. The ROS generation was measured by the increased fluorescence of the DCF dye, which was monitored at an excitation of 485 nm and an emission of 535 nm using a fluorescence plate reader.

4.14. In Vitro Anti-inflammatory Assay. *4.14.1. BSA Denaturation Inhibition Assay.* Inhibition of albumin denaturation was checked by the standard method[64] with slight modification. Five different concentrations of three gold nanocomposites (A, B, and E) were made (200, 400, 600, 800, and 1000 μg/mL) and added to 1.8 mL of 1% BSA solution. The pH was adjusted to 6.5 using 1 N HCl, and the solution was incubated at 37 °C for 20 min and then heated to 57 °C for 10 min. After cooling, turbidity was measured using a UV−vis spectrophotometer at a 660 nm absorbance. Diclofenac sodium was used as the standard, and a solution without a sample/extract was considered as the control. The experiment was done in duplicates. The relative percentage inhibition of protein denaturation was calculated.

$$\%\text{Inhibition} = [(\text{Abs control} - \text{Abs sample})/\text{Abs control}] \times 100$$

4.14.2. Proteinase Inhibition Test. The test was performed according to the modified method of Oyedepo et al. The reaction mixture (2 mL) contained 0.06 mg of trypsin, 1 mL of 20 mM Tris-HCl buffer (pH 7.4), and 1 mL of the test sample that contained the OPD and nanocomposites (A, B, and E) with different concentrations (200, 400, 600, 800, and 1000 μg/mL). The mixture was incubated at 37 °C for 5 min, and then, 1 mL of 0.8% (w/v) casein was added. The mixture was incubated for an additional 20 min. Two milliliters of 70% perchloric acid was added to terminate the reaction. The cloudy suspension was centrifuged, and absorbance of the supernatant was read at 210 nm against the buffer as a blank. The experiment was performed in triplicate.

The percentage inhibition of proteinase inhibitory activity was calculated.

$$\%\text{Inhibition} = (\text{Abs Control} - \text{Abs sample}) \times 100/\text{Abs control}$$

4.14.3. Antilipoxygenase Assay. The antilipoxygenase assay was performed by the following method in ref 64. A total volume of 200 μL of the assay mixture contained 160 μL of sodium phosphate buffer (100 mM, pH 8.0), 10 μL of the OPD and gold nanocomposites (A, B, and E) (200, 400, 600, 800, and 1000 μg extracted material in 100 mM Tris buffer, pH 7.4), and 20 μL of the lipoxygenase enzyme. The mixture containing the plate was shaken for 10 min. The contents were pre-incubated for 10 min at 25 °C. The reaction was initiated by the addition of 20 μL of linoleic acid solution as a substrate. The change in absorbance was observed after 6 min at 234 nm. The reaction mixture stopped after 30 min following the addition of 100 μL of methanol (stop reagent). All reactions were performed in triplicates in a 96-well microplate. A control was made without trypsin treatment. The percentage inhibition (%) was calculated by the following formula

$$\%\text{Inhibition} = [(\text{Abs of the control} - \text{Abs of the test sample})/\text{Abs of the control}] \times 100$$

AUTHOR INFORMATION

Corresponding Authors

Rajlakshmi Devi − *Life Sciences Division, Institute of Advanced Study in Science and Technology, Guwahati 781035, India*; Email: rajiasst@gmail.com

Devasish Chowdhury − *Material Nanochemistry Laboratory, Physical Sciences Division, Institute of Advanced Study in Science and Technology, Guwahati 781035, India*; orcid.org/0000-0003-4829-6210; Phone: +91 361 2912073; Email: devasish@iasst.gov.in; Fax: +91 361 2279909

Author

Kabyashree Phukan − *Material Nanochemistry Laboratory, Physical Sciences Division, Institute of Advanced Study in Science and Technology, Guwahati 781035, India*

Complete contact information is available at: https://pubs.acs.org/10.1021/acsomega.1c00861

Author Contributions

K.P. and D.C. designed the experiments and analyzed the results; K.P. carried out the experiments; D.C., K.P., and R.D. wrote the paper.

https://doi.org/10.1021/acsomega.1c00861
ACS Omega 2021, 6, 17811−17823

Notes

The authors declare no competing financial interest.

■ ACKNOWLEDGMENTS

K.P. wants to thank the Council of Scientific and Industrial Research (CSIR), New Delhi for the fellowship. The authors also thank Mr. Partha Pratim Sarmah and Mr. Simanta Bharwaj for their help.

■ REFERENCES

(1) Chitra, V.; Sharma, S.; Kayande, N. Evaluation of Anticancer Activity of *Vitex negundo* in Experimental Animals: An in Vitro and in Vivo Study. *Int. J. PharmTech. Res.* **2009**, *1*, 1485−1489.

(2) Kulkarni, R. R.; Virkar, A. D.; D'mello, P. Antioxidant and Antiinflammatory Activity of *Vitex negundo*. *Ind. J. Pharm. Sci.* **2008**, *70*, 838−840.

(3) García-Lafuente, A.; Guillamón, E.; Villares, A.; Rostagno, M. A.; Martínez, J. A. Flavonoids as anti-inflammatory agents: implications in cancer and cardiovascular disease. *Inflammation Res.* **2009**, *58*, 537−552.

(4) Anilkumar, M. *Ethnomedicine: A Source of Complementary Therapeutics*; Research signpost: Trivandrum, India, 2010, 267−293, ISBN 978−81−308-0390-6.

(5) Kaneko, T.; Baba, N. Protective effect of flavonoids on endothelial cells against linoleic acid hydroperoxide-induced toxicity. *Biosci., Biotechnol., Biochem.* **1999**, *63*, 323−328.

(6) Kawaii, S.; Tomono, Y.; Katase, E.; Ogawa, K.; Yano, M. Antiproliferative activity of flavonoids on several cancer cell lines. *Biosci., Biotechnol., Biochem.* **1999**, *63*, 896−899.

(7) Sanderson, J.; Mclauchlin, W. R.; Williamson, G. Quercetin inhibits hydrogen peroxide-induced oxidation of the rat lens. *Free Rad. Biol. Med.* **1999**, *26*, 639−645.

(8) Shutenko, Z.; Henry, Y.; Pinard, E.; Seylaz, J.; Potier, P.; Berthet, F.; Girard, P.; Sercombe, R. Influence of the antioxidant quercetin in vivo on the level of nitric oxide determined by electron paramagnetic resonance in rat brain during global ischemia and reperfusion. *Biochem. Pharmacol.* **1999**, *57*, 199−208.

(9) Goldman, I.; Kopelberg, M.; Devaen, J.; Schwartz, B. Antiplatelet activity in onions is sulfur dependent. *Thromb. Haemostasis* **1996**, *73*, 450−452.

(10) Teixeira, S.; Siquet, C.; Alves, C.; Boal, I.; Marques, M. P.; Borges, F.; Lima, J. L. F. C.; Reis, S. Structure-property studies on the antioxidant activity of flavonoids present in diet. *Free Radical Biol. Med.* **2005**, *39*, 1099−1108.

(11) Verri, W. A.; Vicentini, F. T. M. C.; Baracat, M. M.; Georgetti, S. R.; Cardoso, R. D. R.; Cunha, T. M.; Ferreira, S. H.; Cunha, F. Q.; Fonseca, M. J. V.; Casagrande, R. Flavonoids as Anti-Inflammatory and Analgesic Drugs: Mechanisms of Action and Perspectives in the Development of Pharmaceutical Forms. *Stud. Nat. Prod. Chem.* **2012**, *36*, 297−330.

(12) Rushworth, S. A.; Chen, X.-L.; Mackman, N.; Ogborne, R. M.; O'Connell, M. A. Lipopolysaccharide-induced heme oxygenase-1 expression in human monocytic cells is mediated via Nrf2 and protein kinase C. *J. Immunol.* **2005**, *175*, 4408−4415.

(13) Hewett, J. A.; Roth, R. A. Hepatic and extrahepatic pathobiology of bacterial lipopolysaccharides. *Pharmacol. Rev.* **1993**, *45*, 382−411.

(14) Gülsen, A.; Makris, D. P.; Kefalas, P. Biomimetic oxidation of quercetin: isolation of a naturally occurring quercetin heterodimer and evaluation of its in vitro antioxidant properties. *Food Res. Int.* **2007**, *40*, 7−14.

(15) Prakash, D.; Upadhyay, G.; Singh, B. N.; Singh, H. B. Antioxidant and free radical-scavenging activities of seeds and agri-wastes of some varieties of soybean (Glycine max). *Food Chem.* **2007c**, *104*, 783−790.

(16) Prakash, D.; Singh, B. N.; Upadhyay, G. Antioxidant and free radical scavenging activities of phenols from onion (Allium cepa). *Food Chem.* **2007a**, *102*, 1389−1393.

(17) Balasenthil, S.; Arivazhagan, S.; Ramachandran, C. R.; Ramachandran, V.; Nagini, S. Chemopreventive potential of neem (Azadirachta indica) on 7,12- dimethylbenz[a]anthracene (DMBA) induced hamster buccal pouch carcinogenesis. *J. Ethnopharmacol.* **1999**, *67*, 189−195.

(18) Valko, M.; Leibfritz, D.; Moncola, J.; Cronin, M. T. D.; Mazura, M.; Telser, J. Free radicals, and antioxidants in normal physiological functions and human disease. *Int. J. Biochem. Cell Biol.* **2007**, *39*, 44−84.

(19) Liou, G. Y.; Storz, P. Reactive oxygen species in cancer. *Free Radical Res.* **2010**, *44*, 479−496.

(20) Alfadda, A. A.; Sallam, R. M. Reactive oxygen species in health and disease. *J. Biomed. Biotechnol.* **2012**, *2012*, 1−14.

(21) Gaysinsky, S.; Davidson, P. M.; Bruce, B. D.; Weiss, J. Stability and antimicrobial efficiency of eugenol encapsulated in surfactant micelles as affected by temperature and pH. *J. Food Prot.* **2005**, *68*, 1359−1366.

(22) Pralhad, T.; Rajendrakumar, K. Study of freeze-dried quercetin−cyclodextrin binary systems by DSC, FT-IR, X-ray diffraction, and SEM analysis. *J. Pharm. Biomed. Anal.* **2004**, *34*, 333−339.

(23) Lee, S. H.; Zhang, Z.; Feng, S. S. Nanoparticles of poly(lactide)—tocopheryl polyethylene glycol succinate (PLA-TPGS) copolymers for protein drug delivery. *Biomaterials* **2007**, *28*, 2041−2050.

(24) Chen, J.; Ouyang, J.; Kong, J.; Zhong, W.; Xing, M. M. Photo-cross-linked and pH-sensitive biodegradable micelles for doxorubicin delivery. *ACS Appl. Mater. Interfaces* **2013**, *5*, 3108−3117.

(25) Tian, Y.; Chen, J.; Zahtabi, F.; Keijzer, R.; Xing, M. Nanomedicine as an innovative therapeutic strategy for pediatric lung diseases. *Pediatr. Pulmonol.* **2013**, *48*, 1098−1111.

(26) Kasithevar, M.; Saravanan, M.; Prakash, P.; Kumar, M.; Ovais, H.; Barabadi, H.; Shinwari, Z. K. Green synthesis of silver nanoparticles using Alysicarpus monilifer leaf extract and its antibacterial activity against MRSA and CoNS isolated in HIV patients. *J. Interdiscip. Nanomed.* **2017**, *2*, 131−141.

(27) Barabadi, H.; Ovais, M.; Shinwari, Z. K.; Saravanan, M. Anti-cancer green bionanomaterials: Present status and future prospects. *Green Chem. Lett. Rev.* **2017**, *10*, 285−314.

(28) Fakruddin, M.; Hossain, Z.; Afroz, H. Prospects and applications of nanobiotechnology: a medical perspective. *J. Nanobiotechnol.* **2012**, *10*, 31.

(29) Castro-Aceituno, V.; Ahn, S.; Simu, S. Y.; Singh, P.; Mathiyalagan, R.; Lee, H. A.; Yang, D. C. Anticancer activity of silver nanoparticles from Panax ginseng fresh leaves in human cancer cells. *Biomed. Pharmacol.* **2016**, *84*, 158−165.

(30) David, L.; Moldovan, B.; Vulcu, A.; Olenic, L.; Perde-Schrepler, M.; Fischer-Fodor, E.; Florea, A.; Crisan, M.; Chiorean, I.; Clichici, S.; Filip, G. A. Green synthesis, characterization and anti-inflammatory activity of silver nanoparticles using European black elderberry fruits extract. *Colloids Surf., B* **2014**, *122*, 767−777.

(31) Mohanta, Y. K.; Panda, S. K.; Jayabalan, R.; Sharma, N.; Bastia, A. K.; Mohanta, T. K. Antimicrobial, Antioxidant and Cytotoxic Activity of Silver Nanoparticles Synthesized by Leaf Extract of *Erythrina suberosa* (Roxb.). *Front. Mol. Biosci.* **2017**, *4*, 1−9.

(32) Abdel-Aziz, M. S.; Shaheen, M. S.; El-Nekeely, A. A.; Abdel-Wahhab, M. A. Antioxidant and antibacterial activity of silver nanoparticles biosynthesized using Chenopodium murale leaf extract. *J. Saudi Chem. Soc.* **2014**, *18*, 356−363.

(33) Botteon, C. E. A.; Silva, L. B.; Ccana-Ccapatinta, G. V.; Silva, T. S.; Ambrosio, S. R.; Veneziani, R. C. S.; Bastos, J. K.; Marcato, P. D. Biosynthesis and characterization of gold nanoparticles using Brazilian red propolis and evaluation of its antimicrobial and anticancer activities. *Sci. Rep.* **2021**, *11*, 1974.

(34) Wongyai, K.; Wintachai, P.; Maungchang, R.; Rattanakit, P. Exploration of the Antimicrobial and Catalytic Properties of Gold Nanoparticles Greenly Synthesized by Cryptolepis buchanani Roem. and Schult Extract. *J. Nanomater.* **2020**, *2020*, 1−11.

https://doi.org/10.1021/acsomega.1c00861
ACS Omega 2021, 6, 17811−17823

(35) Narayanan, K. B.; Sakthivel, N. Biological synthesis of metal nanoparticles by microbes. *Adv.Colloid Interface Sci.* **2010**, *156*, 1−13.
(36) Maham, M.; Karami-Osboo, R. Extraction of Sulfathiazole from Urine Samples Using Biosynthesized Magnetic Nanoparticles. *Iran J. Pharm. Res.* **2017**, *16*, 462−470.
(37) Gonnelli, C.; Giordano, C.; Fontani, U.; Salvatici, M. C.; Ristori, S. Green Synthesis of Gold Nanoparticles from Extracts of *Cucurbita pepo* L. Leaves: Insights on the Role of Plant Ageing. *Adv. Bionanomater.* **2018**, 155−164.
(38) Aromal, S. A.; Vidhu, V. K.; Philip, D. Green synthesis of well-dispersed gold nanoparticles using Macrotyloma uniflorum. *Spectrochim. Acta A Mol. Biomol. Spectrosc.* **2012**, *85*, 99−104.
(39) Makarov, V. V.; Love, A. J.; Sinitsyna, O. V.; Makarova, S. S.; Yaminsky, I. V.; Taliansky, M. E.; Kalinina, N. O. "Green" nanotechnologies: synthesis of metal nanoparticles using plants. *Acta Nat.* **2014**, *6*, 35−44.
(40) Maensiri, S.; Laokul, P.; Klinkaewnarong, J.; Prokha, S.; Promark, V.; Seraphin, S. Indium oxide (In_2O_3) nanoparticles using Aloe vera plant extract: Synthesis and optical properties *Optoelectron. Adv. Mater.* **2008**, *2*, 161−165.
(41) Kumar, P. S. M.; Ali, D. M.; Saratale, R. G.; Saratale, G. D.; Pugazhendhi, A.; Gopalakrishnan, K.; Thajuddin, N. Synthesis of nano-cuboidal gold particles for effective antimicrobial property against clinical human pathogens. *Microb. Pathog.* **2017**, *113*, 68−73.
(42) Suganthy, N.; Ramkumar, V. S.; Pugazhendhi, A.; Benelli, G.; Archunan, G. Biogenic synthesis of gold nanoparticles from Terminalia arjuna bark extract: assessment of safety aspects and neuroprotective potential via antioxidant, anticholinesterase, and anti-amyloidogenic effects. *Environ. Sci. Pollut. Res. Int.* **2018**, *25*, 10418−10433.
(43) Sanvicens, N.; Marco, M. P. Multifunctional nanoparticles-properties and prospects for their use in human medicine. *Trends Biotechnol.* **2008**, *26*, 425−433.
(44) Singh, P.; Pandit, S.; Mokkapati, V. R. S. S.; Garg, A.; Ravikumar, V.; Mijakovic, I. Gold Nanoparticles in Diagnostics and Therapeutics for Human Cancer. *Int. J. Mol. Sci.* **2018**, *19*, 1979−1999.
(45) Uzma, M.; Vinay, B. R.; Girisha, S. T. Biogenesis of gold nanoparticles, role of fungal endophytes and evaluation of anticancer activity-A review. *Eur. J. Biomed. Pharm. Sci.* **2018**, *5*, 319−329.
(46) Chen, H.; Ng, J. P. M.; Tan, Y.; McGrath, K.; Bishop, D. P.; Oliver, B.; Valenzuela, S. M. Gold nanoparticles improve metabolic profile of mice fed a high-fat diet. *J. Nanobiotechnol.* **2018**, *16*, 11−15.
(47) Kwak, H.-H.; Seo, J. M.; Kim, N.-H.; Arasu, M. V.; Kim, S.; Yoon, M. K.; Kim, S.-J. Variation of quercetin glycoside derivatives in three onions (Allium cepa L.) varieties. *Saudi J. Biol. Sci.* **2017**, *24*, 1387−1391.
(48) Rawat, K. A.; Kailasa, S. K. Visual detection of arginine, histidine, and lysine using quercetin-functionalized gold nanoparticles. *Microchim. Acta* **2014**, *181*, 1917−1929.
(49) Singh, V.; Krishan, P.; Shri, R. Extraction of antioxidant phytoconstituents from onion waste. *Int. J. Pharmacogn. Phytochem. Res.* **2017**, *6*, 502−505.
(50) Lee, K. A.; Kim, K. T.; Kim, H. J.; Chung, M. S.; Chang, P. S.; Park, H.; Pai, H. D. Antioxidant activities of onion (Allium cepa L.) peel extracts produced by ethanol, hot water, and subcritical water extraction. *Food Sci. Biotechnol.* **2014**, *23*, 615−621.
(51) Priyanga, K. S.; Vijayalakshmi, K. Investigation of antioxidant potential of Quercetin and Hesperidin: An In-vitro approach. *Asian J Pharm Clin Res.* **2017**, *10*, 83−86.
(52) Lu, X.; Wang, J.; Al-Qadiri, H. M.; Ross, C. F.; Powers, J. R.; Tang, J.; Rasco, B. A. Determination of total phenolic content and antioxidant capacity of onion (Allium cepa) and shallot (Allium oschaninii) using infrared spectroscopy. *Food Chem.* **2011**, *129*, 637−644.
(53) Singh, B. N.; Singh, B. R.; Singh, R. L.; Prakash, D.; Singh, D. P.; Sarma, B. K.; Upadhyay, G.; Singh, H. B. Polyphenolics from various extracts/fractions of red onion (Allium cepa) peel with potent antioxidant and antimutagenic activities. *Food Chem. Toxicol.* **2009**, *47*, 1161−1167.
(54) Ammulu, M. A.; Viswanath, K. V.; Giduturi, A. K.; Vemuri, P. K.; Mangamuri, U.; Poda, S. Phytoassisted synthesis of magnesium oxide nanoparticles from Pterocarpus marsupium rox.b heartwood extract and its biomedical applications. *J. Genet. Eng. Biotechnol.* **2021**, *19*, 1−18.
(55) Velidandi, A.; Pabbathi, N. P. P.; Dahariya, S.; Baadhe, R. R. Green synthesis of novel Ag−Cu and Ag−Zn bimetallic nanoparticles and their in vitro biological, eco-toxicity and catalytic studies. *Nano-Struct. Nano-Objects* **2021**, *26*, 100687.
(56) Padalia, H.; Chanda, S. Antioxidant and Anticancer Activities of Gold Nanoparticles Synthesized Using Aqueous Leaf Extract of Ziziphus nummularia. *BioNanoScience.* **2021**, *11*, 281−294.
(57) Chinnathambi, A.; Alahmadi, T. A. Zinc nanoparticles green-synthesized by Alhagi maurorum leaf aqueous extract: Chemical characterization and cytotoxicity, antioxidant, and anti-osteosarcoma effects. *Arab. J. Chem.* **2021**, *14*, 103083.
(58) Patra, J. K.; Shin, H. S.; Das, G. Characterization and Evaluation of Multiple Biological Activities of Silver Nanoparticles Fabricated from Dragon Tongue Bean Outer Peel Extract. *Int. J. Nanomed.* **2021**, *16*, 977−987.
(59) Okoli, C. O.; Akah, P. A.; Onuoha, N. J.; Okoye, T. C.; Nwoye, A. C.; Nworu, C. S. Acanthus montanus: An experimental evaluation of the antimicrobial, anti-inflammatory and immunological properties of a traditional remedy for furuncles. *BMC Complementary Altern. Med.* **2008**, *8*, 27.
(60) Kim, J.; Kim, J. S.; Park, E. Cytotoxic and anti-inflammatory effects of onion peel extract on lipopolysaccharide-stimulated human colon carcinoma cells. *Food Chem. Toxicol.* **2013**, *62*, 199−204.
(61) Kumar, A. N.; Bevara, G. B.; Laxmikoteswramma, K.; Malla, R. R. Antioxidant, cytoprotective and anti-inflammatory activities of stem bark extract of Semecarpus anacardium. *Asian J. Pharm. Clin. Res.* **2013**, *6*, 213−219.
(62) Govindappa, M.; Naga, S. S.; Poojashri, M. N.; Sadananda, T. S.; Chandrappa, C. P. Antimicrobial, antioxidant, and in vitro anti-inflammatory activity of ethanol extract and active phytochemical screening of Wedelia trilobata (L.) Hitchc. *J. Pharmacogn. Phytother.* **2011**, *3*, 43−51.
(63) Das, S. N.; Chatterjee, S. Long term toxicity study of ART-400. *Indian Indy Med.* **1995**, *16*, 117−123.
(64) Jyothilakshmi, M.; Jyothis, M.; Latha, M. S. Cyclooxygenase, Lipoxygenase, Nitric Oxide Synthase, Myeloperoxidase and Protease Inhibiting Activities of the Leaves and Flowers of *Mikania micrantha Kunth*. *J. Complement. Med. Res.* **2020**, *11*, 51−59.
(65) Truong, D. H.; Ta, N. T. A.; Pham, T. V.; Huynh, T. D.; Do, Q. T. G.; Dinh, N. C. G.; Dang, C. D.; Nguyen, T. K. C.; Bui, A. V. Effects of solvent-solvent fractionation on the total terpenoid content and in vitro anti-inflammatory activity of *Serevenia buxifolia* bark extract. *Food Sci. Nutr.* **2021**, *9*, 1720−1735.
(66) Zeraik, M. L.; Pauli, I.; Dutra, L. A.; Cruz, R. S.; Valli, M.; Paracatu, L. C.; de Faria, C. M. Q. G.; Ximenes, V. F.; Regasini, L. O.; Andricopulo, A. D.; Bolzani, V. S. Identification of a Prenyl Chalcone as a Competitive Lipoxygenase Inhibitor: Screening, Biochemical Evaluation and Molecular Modeling Studies. *Molecules* **2021**, *26*, 2205.

https://doi.org/10.1021/acsomega.1c00861
ACS Omega 2021, 6, 17811−17823